The EMBO Journal (2011) 30, 3004–3018 | © 2011 European Molecular Biology Organization | Some Rights Reserved 0261-4189/11
www.embojournal.org

THE EMBO JOURNAL

EMBO open

TCF/Lef1 activity controls establishment of diverse stem and progenitor cell compartments in mouse epidermis

Monika Petersson[1], Heike Brylka[1], Andreas Kraus[1], Susan John[1], Gunter Rappl[2], Peter Schettina[1] and Catherin Niemann[1,*]

[1]Center for Molecular Medicine Cologne (CMMC), Institute of Pathology, University of Cologne, Cologne, Germany and [2]Department of Internal Medicine 1, University of Cologne, Cologne, Germany

Mammalian epidermis consists of the interfollicular epidermis, hair follicles (HFs) and associated sebaceous glands (SGs). It is constantly renewed by stem and progenitor cell populations that have been identified and each compartment features a distinct mechanism of cellular turnover during renewal. The functional relationship between the diverse stem cell (SC) pools is not known and molecular signals regulating the establishment and maintenance of SC compartments are not well understood. Here, we performed lineage tracing experiments to demonstrate that progeny of HF bulge SCs transit through other SC compartments, suggesting a hierarchy of competent multipotent keratinocytes contributing to tissue renewal. The bulge was identified as a bipotent SC compartment that drives both cyclic regeneration of HFs and continuous renewal of SGs. Our data demonstrate that aberrant signalling by TCF/Lef1, transcription factors crucial for bulge SC activation and hair differentiation, results in development of ectopic SGs originating from bulge cells. This process of *de novo* SG formation is accompanied by the establishment of new progenitor niches. Detailed molecular analysis suggests the recapitulation of steps of tissue morphogenesis.

The EMBO Journal (2011) **30,** 3004–3018. doi:10.1038/emboj.2011.199; Published online 21 June 2011
Subject Categories: signal transduction; development
Keywords: epidermis; Lef1; sebaceous gland; skin; stem cell

Introduction

Adult stem cells (SCs) are essential for skin homoeostasis and the repair of damaged tissue following injury. Renewal of the epidermis is maintained by multipotent SCs capable to generate all differentiated lineages of the tissue including the interfollicular epidermis (IFE), hair follicles (HFs) and sebaceous glands (SGs) (Niemann and Watt, 2002; Fuchs and Horsley, 2008). Each of these lineages features a distinct mechanism of cellular turnover and tissue renewal. In contrast to continuous renewal of the IFE and SG, HF regeneration is a highly dynamic and cyclic process (Alonso and Fuchs, 2006). HFs undergo distinct phases of growth (anagen), regression (catagen) and rest (telogen), thereby facilitating the formation of a new hair that will be replaced during the following hair cycle. Previously, several signals governing HF morphogenesis and regulation of the hair cycle have been unravelled (Watt *et al*, 2006; Blanpain and Fuchs, 2009).

Keratinocytes of the IFE, HF and SG fulfil different functions to ensure tissue integrity, barrier acquisition and hydration of the skin. As an integral part of the pilosebaceous unit, the SG is attached to the HF. SGs produce and secrete sebum and specific SG function depends on proper differentiation of sebocytes followed by the process of holocrine secretion (Zouboulis *et al*, 2008; Schneider and Paus, 2009). To date, the molecular and cellular mechanisms underlying morphogenesis and regeneration of the SG are barely understood. Currently, two hypotheses are discussed how SGs are maintained on a cellular level: (1) renewal is independent of the HF and residing unipotent progenitor cells located at the periphery of the SG are committed to the sebaceous lineage (Ghazizadeh and Taichman, 2001; Horsley *et al*, 2006; Jensen *et al*, 2009) or (2) HF SCs are mobilised to renew the SG (Panteleyev *et al*, 2000; Taylor *et al*, 2000; Morris *et al*, 2004; Snippert *et al*, 2010). Indeed, SCs of the HF bulge region have long been appreciated as an important reservoir for constant renewal of the HF throughout adult life and the regeneration of epidermal tissue after injuries (Cotsarelis *et al*, 1990; Ito *et al*, 2005; Blanpain and Fuchs, 2009). HF SCs have been purified based on the expression of the following marker molecules: CD34/α6-integrin (Trempus *et al*, 2003; Blanpain *et al*, 2004), Lgr5 (Jaks *et al*, 2008), Keratin 15 (K15) (Morris *et al*, 2004) and label retention representing a slow cycling keratinocyte population (Cotsarelis *et al*, 1990; Tumbar *et al*, 2004). Furthermore, bulge cells have been distinguished by certain SC markers including Sox9, Lhx2, NFATc1 and Tcf3 (Figure 1A; Merrill *et al*, 2001; Vidal *et al*, 2005; Rhee *et al*, 2006; Horsley *et al*, 2008; Nowak *et al*, 2008).

Additionally, stem and progenitor cell populations residing above the HF bulge have been identified (Figure 1A). One cell population, which is recognised by the MTS24 antibody, is located in the upper isthmus (UI) of the HF. It does not express the HF bulge markers K15 and CD34, but is clonogenic *in vitro* (Nijhof *et al*, 2006). The epitope for MTS24 has recently been identified to correspond to Plet1, a glycosylphosphatitylinositol-anchored glycoprotein that is also expressed by more differentiated keratinocytes of hair lineages (Depreter *et al*, 2008; Raymond *et al*, 2010). Another SC population of the UI region expresses low levels of α6-integrin

*Corresponding author. Center for Molecular Medicine Cologne (CMMC), University of Cologne, CMMC Research Building, Robert-Koch-Strasse 21, Cologne D-50931, Germany.
Tel.: +49 221 47889511; Fax: +49 221 47886737;
E-mail: cnieman1@uni-koeln.de

Received: 2 March 2011; accepted: 25 May 2011; published online: 21 June 2011

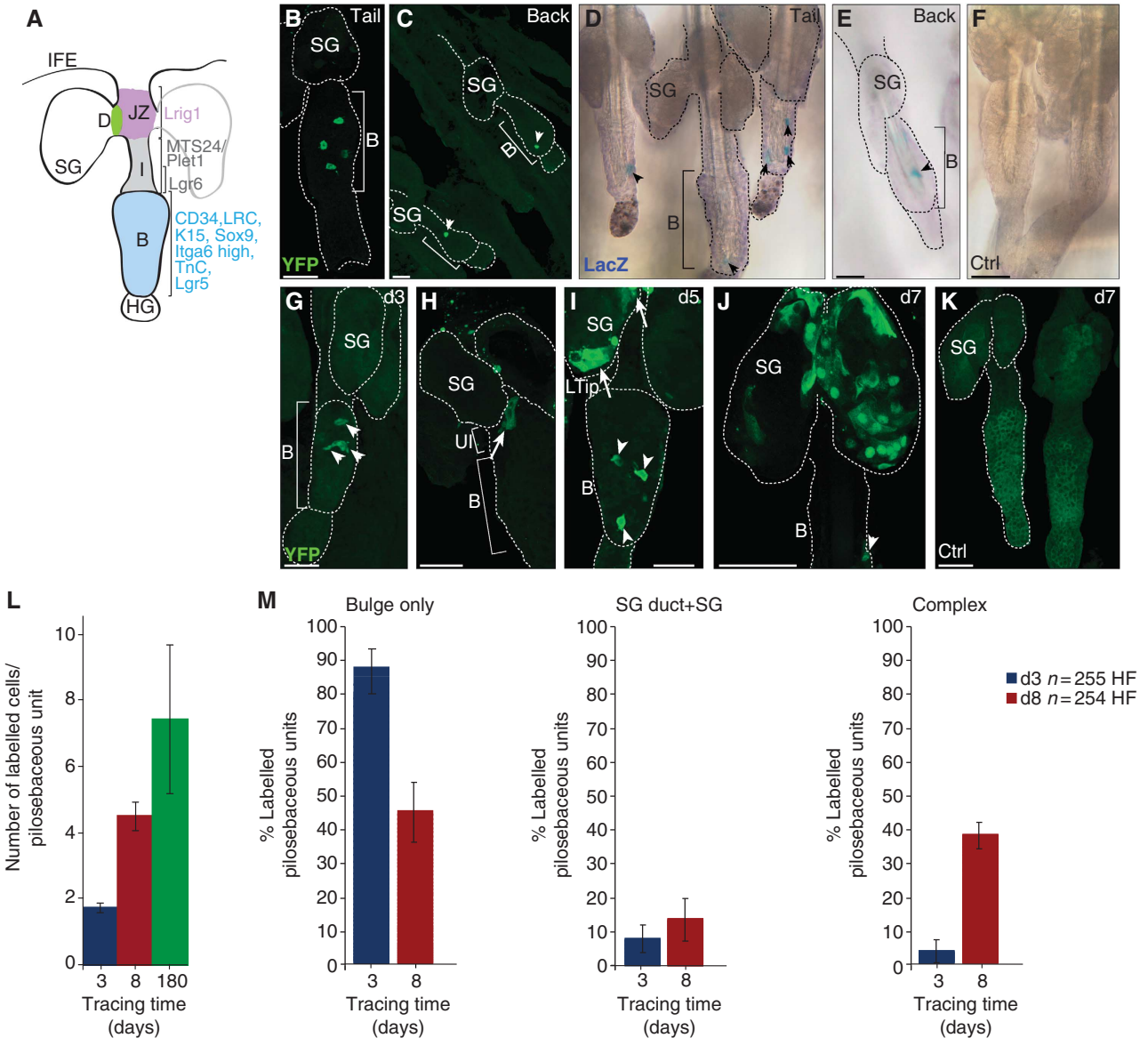

Figure 1 HF bulge-derived SCs reconstitute SGs. (**A**) Scheme of marker molecules identified for different stem and progenitor populations within the murine pilosebaceous unit. (**B**–**K**) Epidermal whole mounts of A_K15CreER^{low}/R26R-reporter mice following Tam (**B**–**E**, **G**–**J**) or vehicle administration (**F**, **K**) during telogen. Detection of YFP (**B**, **C**) and LacZ (**D**, **E**) in tail (**B**, **D**) or back skin (**C**, **E**) in the HF bulge 3 days after Tam pulse. Chasing of YFP+ SC progeny in epidermal whole mounts at 3 (**G**), 5 (**H**, **I**) and 7 days (**J**) after Tam administration. No specific YFP and LacZ signal in vehicle controls (**F**, **K**). Scale bars, 50 μm. B, bulge; D, SG duct; HG, hair germ; JZ, junctional zone; LTip, lower tip of the SG; SG, sebaceous gland; UI, upper isthmus. (**L**) Total number of labelled cells in pilosebaceous units determined at 3 (blue bar, $n=255$ HF), 8 (red bar, $n=254$ HF), and 180 (green bar, $n=178$ HF) days after Cre activation ($n=3$ mice/time point). (**M**) Statistical analyses of lineage-traced bulge progeny for frequency and location of LacZ+ keratinocytes grouped into: Bulge only, SG duct+SG only and Bulge+SG duct+SG (Complex) shown as average with s.d. ($n=3$ mice/time point).

and lacks CD34 and Sca-1 expression (Jensen *et al*, 2008). These SCs are multipotent but are distinguished by a gene expression profile that is different from SCs of the HF bulge. More recently, the upper region adjacent to the HF bulge has been shown to be positive for Lgr6, a heterotrimeric guanine nucleotide-binding protein-coupled receptor and close relative to the *Lgr5* gene. Snippert *et al* (2010) report contribution of multipotent Lgr6+ keratinocytes to the SG and IFE. However, it is not known if the Lgr6 SC pool overlaps with the compartment lacking CD34 and Sca-1 expression. In addition, a population positive for the transmembrane protein Lrig1, a marker for SCs of the human IFE, constitutes a multipotent SC compartment located in the junctional zone (JZ) between UI and IFE adjacent to the SG. Interestingly, Jensen *et al* (2009) suggested that these JZ SCs are bipotent, replenishing the IFE and SG, but not the HF lineages. The transcriptional repressor Blimp1 has been proposed to be a marker of SG progenitor cells controlling SG homoeostasis by regulating expression of c-myc (Horsley *et al*, 2006). The recent discovery of these distinct and multipotent cell populations of the pilosebaceous unit provokes the question for their functional significance and if they function autonomously under physiological conditions during tissue homoeostasis.

One important signalling pathway controlling SC function is the Wnt pathway. Canonical Wnt/β-catenin signalling is

crucial for SC maintenance, proliferation and directing cell fate decisions in many different organs (Clevers, 2006; Wend *et al*, 2010). In adult skin, transcription factors Tcf3 and Lef1 are important mediators of β-catenin signalling governing bulge SC activation for hair renewal and HF differentiation (Niemann, 2006; Haegebarth and Clevers, 2009). In contrast, inhibition of TCF/Lef1 activity seems to be an important prerequisite enabling progenitor cells to promote SG differentiation (Niemann *et al*, 2002; Han *et al*, 2006). However, it is not known where determination of cell fate actually occurs within the tissue and if regulation of TCF/Lef1 activity within the bulge SCs is sufficient to control cell fate commitment.

Our study addresses important new aspects of SC function in a dynamic and complex epithelial tissue. Here, we investigate if HF bulge SCs are able to give rise to other stem and progenitor cell compartments of the pilosebaceous unit. We ask whether HF bulge cells are able to respond to various distinct molecular signals by renewing different cellular compartments within the tissue. Additionally, we analyse the molecular mechanisms underlying the process of tissue regeneration by SCs and perform live cell imaging of bulge SCs to study the cellular mechanisms of tissue renewal more precisely. Furthermore, the molecular function of TCF/Lef1 signalling in epidermal regeneration by SCs of the HF bulge was investigated in detail. Finally, the bulge SC compartment was manipulated *in vivo* by interfering with TCF/Lef1 signalling activity to demonstrate that cell fate determination already proceeds within SCs and their direct progeny.

Results

HF bulge cells contribute to SG renewal during skin homoeostasis

To understand the relation between HF bulge SCs and other progenitor and committed cell populations, we genetically labelled bulge cells during telogen and analysed the distribution of progeny during skin homoeostasis. We generated K15CreER(G)T2 transgenic mouse lines with epithelial expression of the Tam (tamoxifen) inducible CreER(G)T2 (Indra *et al*, 1999) under control of the K15 regulatory promoter sequence (Liu *et al*, 2003; Morris *et al*, 2004; Ito *et al*, 2005). K15CreER(G)T2 mouse lines were crossed with R26RYFP and R26RLacZ Cre-reporter mice (Soriano, 1999; Srinivas *et al*, 2001). Tam administration results in YFP or β-galactosidase expression in HF bulge cells and all descending cell lineages, respectively. To screen large areas of the skin in a three-dimensional manner, epidermal whole mounts of mouse tail and back skin were analysed for YFP/LacZ+ cells (Braun *et al*, 2003). Consistent with previous reports (Lyle *et al*, 1999; Liu *et al*, 2003), we identified a population of LacZ+ cells that constitutes almost the entire HF bulge region in one founder line strongly expressing the transgene (C_K15CreER^{high}) (Supplementary Figure S1A and B; Morris *et al*, 2004; Youssef *et al*, 2010). A different founder line (A_K15CreER^{low}) exhibited low expression levels of the transgene and individual cells could be targeted by Tam administration (Figure 1B–E; Supplementary Figure S1D). Importantly, a negligible number of YFP+ cells were seen within the IFE at 3 days following Cre activation (Supplementary Figure S1E). The bulge-specific pattern of Cre activation in both lines was confirmed by immunostaining for nuclear localisation of active Cre enzyme (Supplementary Figure S1B and C). In contrast, control mice treated with oil vehicle alone did not show nuclear localisation of Cre protein and were negative for YFP or LacZ (Figure 1F and K; Supplementary Figures S1A, B and D and S2J and K).

Subsequently, the low expressing Cre line (A_K15CreER^{low}) was utilised as a powerful tool to map the fate of individual bulge SCs. Whole mounts of adult tail epidermis were analysed at different time points after Cre activation in synchronous telogen hair cycle phase. Over 50% of HFs were labelled and individual YFP+ cells were detected specifically in the HF bulge within 2–3 days following Tam administration (Figure 1B and G). In contrast, 5 days after Cre activation labelled cells also appeared in the UI and the SG duct (Figure 1H). At day 5 following Cre activation, bulge progeny were also found at the lower tip of the SG (Figure 1I) and after a chasing time of 7 days almost the entire SG comprised YFP+ bulge progeny (Figure 1J). Similar results were obtained with a LacZ-reporter line (Supplementary Figure S1D). Individual bulge cells were targeted by Cre recombinase also in back skin and labelling frequency was lower in follicles within back skin when compared with those in tail epidermis (Figure 1B–E). This revealed that labelling bulge cells in A_K15CreER^{low} mice is not restricted to a specific skin region. Importantly, bulge progeny were also found to repopulate SGs in back skin, indicating that renewal of the SG by HF bulge SCs constitutes a more general mechanism.

Statistical analyses of tracing experiments were performed to quantify the distribution and frequency of labelled cells during telogen. Counting the total number of labelled cells within the pilosebaceous unit revealed an overall increase from 1.7 positive cells seen at day 3 to 4.5 labelled cells at day 8 following Cre activation (Figure 1L). At 3 days of tracing, the majority of LacZ+ HF (88.5%) was identified with a 'bulge only' distribution (Figure 1M). Eight days after Tam administration, a decrease in HFs exhibiting LacZ+ keratinocytes within the 'bulge only' occurs in conjunction with a strong increase in number of pilosebaceous units possessing a more complex pattern with LacZ+ cells in the bulge, SG duct and SG (40%). The region of the SG duct was defined to the junction between SG and JZ of the HF. Concomitantly, an elevated number of labelled bulge progeny was observed in the SG and SG duct (Figure 1J and M). These data clearly indicate that the HF bulge contains a population of multipotent SCs contributing to the renewal of the SG during skin homoeostasis. Furthermore, the results also show that many LacZ+ cells remain in the HF bulge to replenish the SC pool or to become activated at a later time point.

Three-dimensional reconstructions of whole mounts were performed to visualise size and expansion of labelled cell clones in A_K15CreER^{low}/R26RYFP mice in more detail (Clayton *et al*, 2007; Doupé *et al*, 2010). Interestingly, labelled SC derivates transit the UI and JZ (Figure 2A–D) indicating cell migration. A contiguous trail of YFP+ cells from the HF bulge towards the SG was not seen during the resting phase of the hair cycle. Eventually, labelled bulge progeny repopulate the SG to replenish the tissue (Figure 2E–G). To examine the expansion of labelled cells more precisely, the number of labelled cells (clone size) within different compartments was determined at 3, 8 and 180 days of tracing. There is an increase in the number of positive cells within the bulge

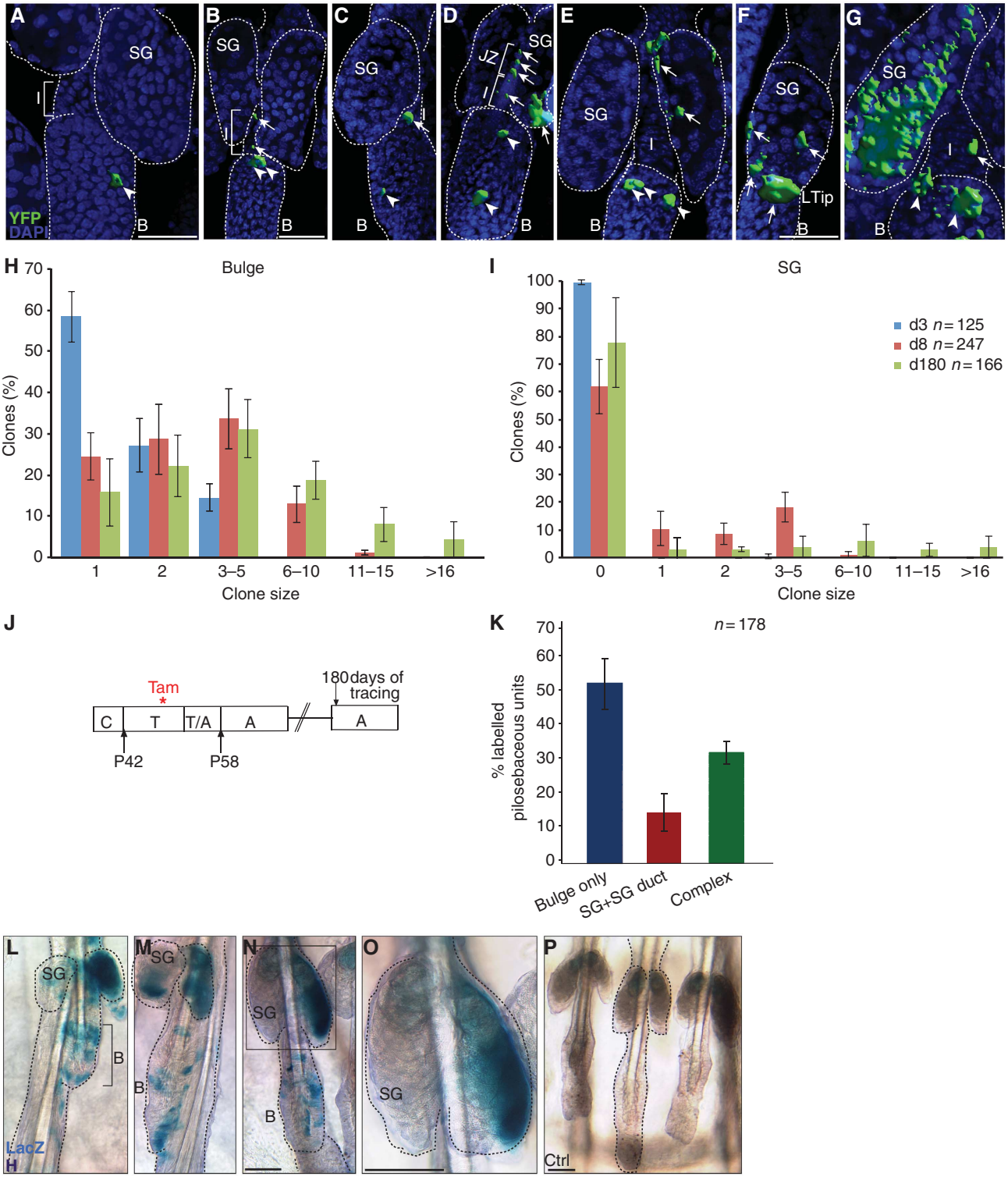

Figure 2 Clonal analysis and long-term studies of HF SC progeny. (**A–G**) Three-dimensional projections of whole-mount reconstructions, illustrating localisation and morphology of YFP+ cell clones with DAPI as nuclear counter stain. (**H**, **I**) Statistical analysis of labelled keratinocytes in A_K15CreER^{low} mice according to the size of clones (number of labelled cells) within the HF bulge (**H**) and SG (**I**) at 3, 8 and 180 days after Cre activation. (**J**) Scheme of Tam administration in A_K15CreER^{low}/R26RLacZ mice and analysis 6 months following treatment. (**K**) Statistical analyses of lineage-traced bulge progeny for frequency and location of LacZ+ keratinocytes grouped into: Bulge only, SG duct + SG only and Bulge + SG duct + SG (Complex) shown as average with s.d. ($n = 3$ mice). (**L–P**) Replenishments of SC pool in HF bulge (**L–N**) and renewal of SGs by LacZ+ bulge progeny (**L–O**). Control mice treated with vehicle (**P**). Scale bars, 50 μm.

(Figure 2H), SG (Figure 2I), JZ (Supplementary Figure S5E) and SG duct (Supplementary Figure S5F) at 8 days following Cre activation compared with the 3-day time point.

To test for recombination events in isthmus progenitor cells of induced A_K15CreER^{low}/R26RYFP mice resulting in a delayed expression of YFP, we sorted α6-integrin+ primary

keratinocytes expressing either CD34 (bulge) or Plet1/MTS24 (isthmus) (Supplementary Figure S2A–H). These different cell populations were investigated for DNA recombination events within the Rosa26 locus by PCR. As demonstrated in Supplementary Figure S2I, excision of the stop cassette upstream of YFP takes only place in CD34+ bulge cells, but not in isthmus progenitor cells at day 2 following Cre activation. In contrast, DNA recombination is detected in bulge cells and isthmus progenitors 6 days following activation of Cre enzyme (Supplementary Figure S2I). These data reveal that the A_K15CreER^{low} mice do not primarily target isthmus progenitor cells. Taken together, we conclude that the SG is defined by a high cellular turnover and that individual YFP+ cells of the HF bulge are multipotent and competent to sustain SG renewal during skin homoeostasis.

SG renewal by multipotent HF bulge cells is continuous and occurs independent of HF regeneration

HF regeneration requires a cyclic activation, mobilisation of bulge SCs and migration of their progeny towards the newly forming hair germ at the tip of the HF bulb (Muller-Rover *et al*, 2001; Cotsarelis, 2006). Once outside the niche, HF bulge-derived cells are destined to a fate of rapid proliferation and differentiation during anagen phase of the hair cycle. Anagen is followed by regression in catagen and telogen. With the transition from telogen to anagen, the HF enters a new cycle, a process being recapitulated throughout adult life (Muller-Rover *et al*, 2001; Greco *et al*, 2009; Zhang *et al*, 2009).

To address the question if the process of SG renewal by HF bulge cells is connected to distinct phases of cyclic HF regeneration (Supplementary Figure S3A), A_K15CreER^{low}/R26RYFP mice were treated with Tam during distinct stages of the synchronised hair cycle. As expected, administration of Tam during telogen to anagen transition resulted in YFP-labelled cells participating in HF regeneration (Supplementary Figure S3B–D). YFP+ bulge progeny were detected in all different hair lineages, including the ORS, layers of the inner root sheath, the hair shaft and the hair germ (Supplementary Figure S4A–D). Importantly, bulge progeny could also be localised in the SG 3 and 6 days following Cre activation (Supplementary Figure S3C and D). This indicates that activation of HF SCs that drive renewal of the SG proceeds concomitantly with the stimulation of bulge progeny for HF regeneration. Interestingly, lineage tracing experiments during telogen to anagen transition revealed that the overall size of individual labelled clones of keratinocytes within the SG is increased (Supplementary Figure S4J) compared with the clone size measured during telogen (Figure 2I). This indicates that activation and mobilisation of bulge SC for HF renewal also leads to an increase in SG renewal by bulge cells. These findings were supported by three-dimensional reconstructions of whole mounts displaying a trail of YFP+ cells expanding from the bulge towards the JZ, SG and HF (Supplementary Figure S4E–G).

SC progeny participated in SG regeneration after going through yet another hair cycle (Supplementary Figures S3E–G and S4H and I). Finally, we activated Cre recombinase at the beginning of anagen when mobilisation of bulge cells for HF growth is completed (Supplementary Figure S3H). Bulge progeny could easily be detected at the periphery and the lower tip of the SG by days 3 to 5 of tracing (Supplementary Figure S3I and J) and subsequently, within the SG after 5 to 7 days of tracing (Supplementary Figure S3K). Taken together, these experiments reveal that SGs are renewed by HF bulge cells at different phases of the hair cycle. Clearly, SCs of the HF bulge are competent to contribute to both HF and SG renewal during tissue homoeostasis.

Replenishment of the bulge SC compartment and SG renewal in long-term studies

Long-term tracing studies were performed to investigate if the labelled HF bulge cells have the potential to regenerate different lineages of the pilosebaceous unit even after 6 months of tracing (Figure 2J). Interestingly, the HF bulge contained an elevated number of LacZ+ keratinocytes compared with initial labelling and tracing events (days 3 and 8; Figure 2H and L–N). Additionally, the size of labelled bulge clones was increased at 180 days after Tam treatment when compared with the earlier tracing time points (days 3 and 8; Figure 2H). This demonstrates that in addition to their activation for tissue regeneration, labelled bulge cells are able to replenish the HF SC pool over longer time periods. It also suggests that bulge SCs are propagated in adult skin and a symmetric cell fate decision takes place generating two multipotent daughter cells. Furthermore, our data demonstrate that no exhaustion of the labelled bulge cells takes place. Importantly, no LacZ+ keratinocytes were observed after 6 months of tracing in control litter mates treated with oil, thereby excluding unspecific activation of Cre enzyme in aging skin (Figure 2P). Many SGs still contained labelled cells, indicating that HF bulge progeny were able to regenerate SGs even after 6 months of tracing (Figure 2K–O). In addition, an increase in the number of labelled cells was detected within the bulge, the SG (Figure 2H and I) and the SG duct (Supplementary Figure S5F) in long-term tracing experiments when compared with earlier time points of analysis. In contrast, no changes in the number of labelled cells were seen within the JZ (Supplementary Figure S5E) and in the total number of LacZ+ SGs at these late stages of the experiment when compared with day 8 after Cre activation (Figures 1L and M and 2K). These results prove that multipotent HF SCs are an important source for constant renewal of SGs over a long time period.

Aberrant Lef1 signalling promotes ectopic SG formation originating in HF bulge cells

In mammalian skin, canonical Wnt/β-catenin signalling has strongly been associated with cell fate determination by stem and progenitor cells (Blanpain and Fuchs, 2006; Niemann, 2006). Particularly, an active β-catenin/Lef1 transcriptional complex is required for HF morphogenesis and hair differentiation. Conversely, disturbed Lef1 signalling results in alteration of the differentiation programme in keratinocytes promoting sebocyte differentiation (Merrill *et al*, 2001; Niemann *et al*, 2002). To date, it is not known whether the development of these ectopic SGs originates from HF SCs or more specified and lineage committed keratinocytes. To address this issue, A_K15CreER^{low}/R26RYFP mice were crossed with K14ΔNLef1 transgenic mice expressing a dominant negative Lef1 transcription factor under control of the keratin 14 promoter (Niemann *et al*, 2002). Cre was activated during telogen and the fate of labelled bulge cells was monitored. Notably, CD34, K15 and α6-integrin showed an abnormal

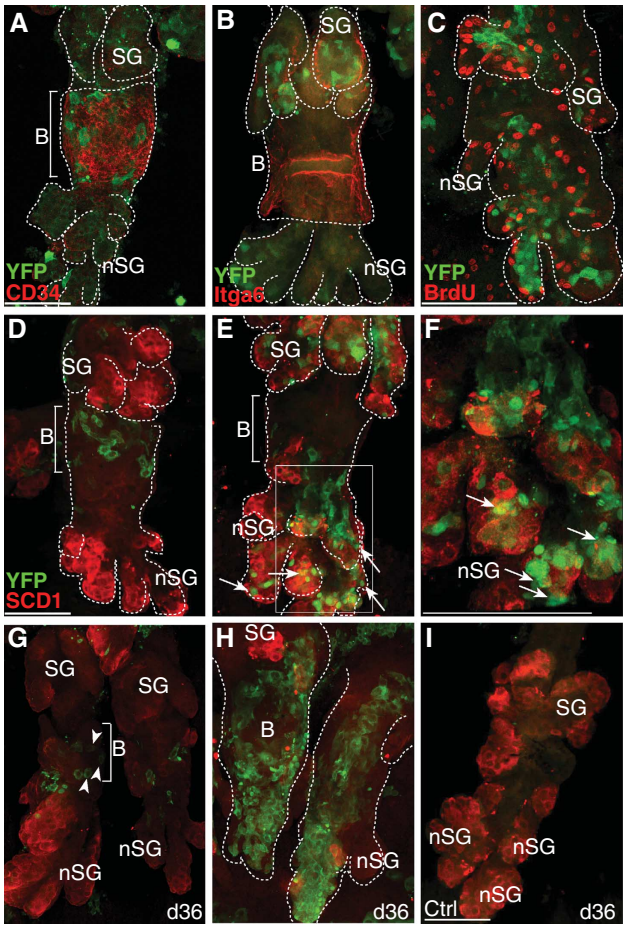

Figure 3 HF bulge progeny constitute ectopic SGs. (**A**–**C**) Detection of bulge marker CD34 (**A**), α6-integrin (**B**, Itga6), BrdU (**C**) and YFP-labelled keratinocytes in deformed HF structures of A_K15CreER^{low}/K14ΔNLef1/R26RYFP mice. (**D**–**I**) Starting with a cluster of YFP+ keratinocytes within the bulge of deformed HFs 3 days after activation (**D**), HF bulge-derived progeny localises to ectopic SGs (**E**, nSG, arrows) and are positive for SCD1 (red) after 5 days following Cre activation (**E**, **F**, arrows). Chasing for 36 days results in labelled resident bulge SCs (**G**, arrow heads) and clonal expansion of bulge progeny in deformed HFs at sites of *de novo* SGs (**H**, nSG). A_K15CreER^{low}/K14ΔNLef1/R26RYFP mice treated with vehicle as control (**I**). Scale bars, 50 μm.

expression pattern in whole mounts of K14ΔNLef1 mice, indicating that the bulge region is changed morphologically (Figures 3A and B and 6A).

At 3 days following Tam treatment, clusters of YFP+ keratinocytes localised to the bulge area of the deformed HFs (Figure 3D), demonstrating that the K15 promoter is still active in the deformed HF bulge of K14ΔNLef1 mice. In contrast, by day 7 of tracing, SC progeny have largely contributed to the deformed HF structures (Figure 3E). The dramatic increase in labelled cells is consistent with our previous finding that ΔNLef1 is promoting cell growth in mammalian skin (Figure 3C; Niemann *et al*, 2002; Niemann *et al*, 2007). Clusters of YFP+ cells were frequently detected within enlarged SGs and at sites of *de novo* formed SGs coexpressing the sebocyte marker SCD1 (Figure 3E and F; Supplementary Figure S6L). Tracing of HF bulge-derived progeny in K14ΔNLef1 mice over a time period of up to 36 days revealed two different patterns of labelled cells. YFP+ keratinocytes were detected in small aggregates confined to the deformed HF bulge, indicating that labelled bulge cells are able to replenish the HF SC niche during long time studies in K14ΔNLef1 mice (Figure 3G). However, in most cases, HF bulge progeny could be observed as large cell clusters along the deformed pilosebaceous units, demonstrating a continuous contribution of HF bulge cells to ectopic SGs (Figure 3H). In contrast, no YFP+ keratinocytes were detected in litter mates treated with vehicle as a control (Figure 3I). These results clearly demonstrate that HF SCs not only regenerate SGs during skin homoeostasis but also participate in *de novo* formation of ectopic SGs in K14ΔNLef1 transgenic mice.

HF bulge progeny transit through distinct stem and progenitor cell compartments

Several multipotent and unipotent progenitor populations residing above the HF bulge have been identified recently (Figure 1A; Nijhof *et al*, 2006; Horsley *et al*, 2006; Jensen *et al*, 2008, 2009; Snippert *et al*, 2010). Since we found labelled HF bulge progeny migrating into this area, we asked about the relationship between the HF bulge and the diverse progenitor pools. We thus analysed YFP+ keratinocytes for the expression of stem and progenitor cell markers in the process of SG renewal. As expected, initially labelled keratinocytes were strongly positive for bulge markers including K15, CD34 and Tenascin C at 3 days after Tam administration (Figure 4A–C). In addition, label retaining cells (LRC) of the HF bulge were also YFP+, demonstrating that Cre activity was also confined to the slow cycling SC compartment of the HF (Figure 4D). Changes in the expression pattern of stem and progenitor cell markers were observed after 5 days of tracing. YFP+ cells were seen within the Plet1/MTS24 compartment at the UI (Figure 4G; Supplementary Figure S5B). In addition, labelled keratinocytes at the periphery of the SG were also positive for Lrig1 (Figure 4H–J; Supplementary Figure S5A). Notably, with increasing tracing time, YFP+ cells are found within the SG and are positive for SCD1, a marker for mature sebocytes (Figure 4K; Supplementary Figure S5C).

Interestingly, some symmetrically grouped LRCs and their descendants are also YFP+. Consistent with our results, proliferating progeny of LRCs are found above the bulge region, indicating that HF SC progeny are indeed expanding to replenish the SG (Figure 4F; Braun *et al*, 2003; Nijhof *et al*, 2006; Zhang *et al*, 2010).

In order to quantify alterations in marker expression of YFP-labelled SC progeny, FACS analysis of YFP+ primary keratinocytes was performed. As expected, there was an overall increase of YFP/α6-integrin expressing cells by 2.9-fold when comparing keratinocytes at 5 and 2 days after Tam administration. Furthermore, a slight increase in YFP+ cells within the α6-integrin+/CD34+ bulge compartment was observed. However, the strongest elevation in number of YFP-expressing keratinocytes was seen within the α6-integrin+/Lrig1 (2.5-fold) and Plet1/MTS24 (2.3-fold) cell pool (Figure 4L).

To analyse genetically labelled cells for expression of lineage markers, primary keratinocytes double positive for α6-integrin and YFP were isolated after 2 and 6 days following Cre activation and compared with α6-integrin^{high}/CD34+ or MTS24+ cells by qRT–PCR (Figure 4M; Supplementary Figure S2A–H). Expression of the sebocyte progenitor marker

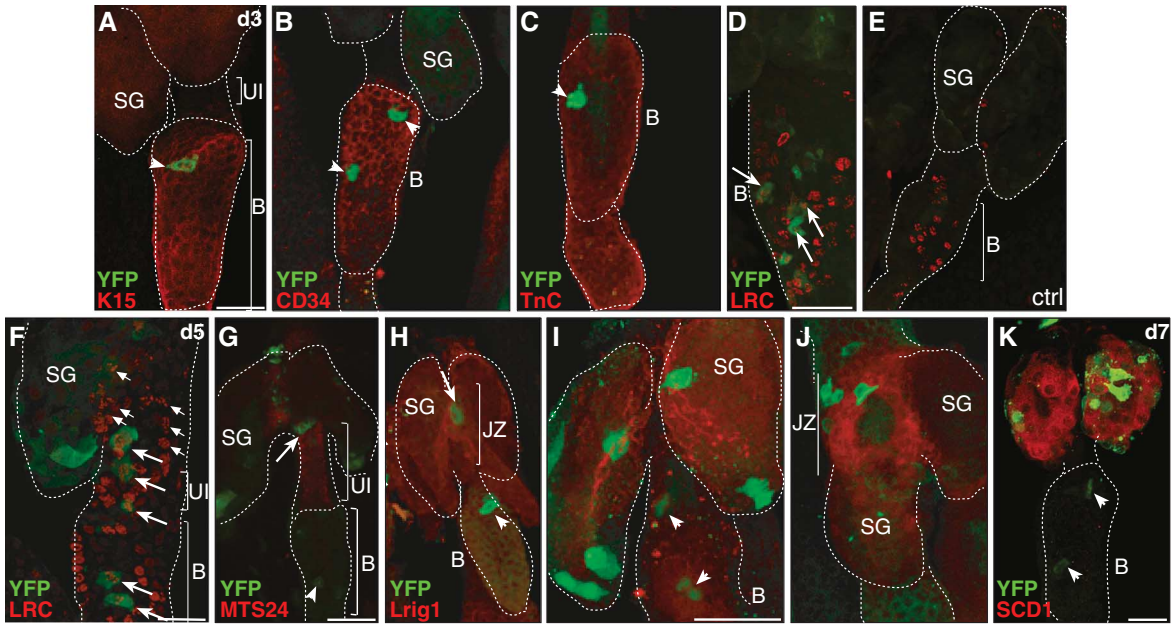

L

Sort	Fold change d5/d2
Itga6	2.9
CD34	1.7
Lrig1	2.5
MTS24	2.3

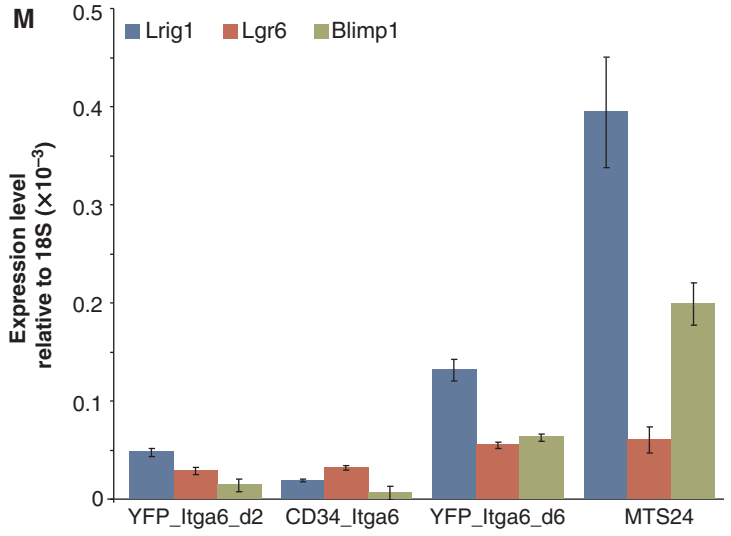

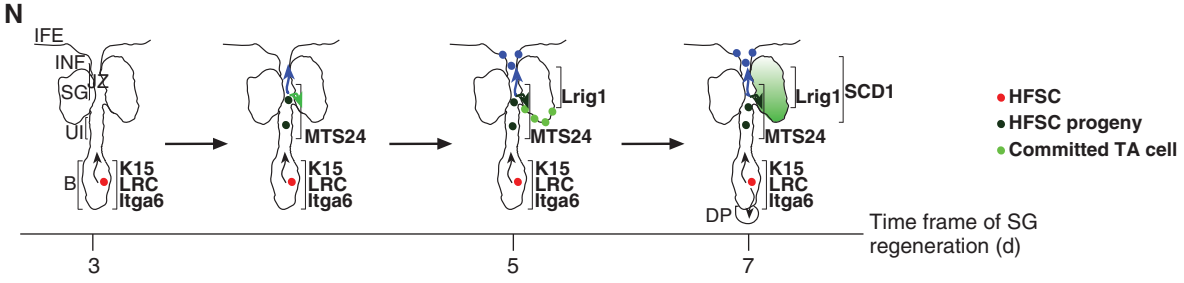

Figure 4 HF bulge progeny transit distinct stem and progenitor cell compartments before differentiating into sebocytes. (**A**–**F**) A_K15CreER^{low}/Rosa26RYFP mice analysed for YFP expression in the HF bulge and colocalisation with K15 (**A**), CD34 (**B**), Tenascin C (**C**) and LRCs (**D**) at 3 days after Tam pulse (**A**–**D**, arrowheads). LRC in HF of vehicle-treated control mice (**E**). LRCs positive for YFP are also dividing at 5 days of chase (**F**). (**G**–**J**) YFP+ bulge progeny transit the MTS24-labelled compartment (**G**) and are positive for Lrig1 (H, higher magnification in **I**, **J**) at 5 to 7 days following Cre activation. (**K**) At day 7 after Tam pulse, YFP+ keratinocytes are positive for the SG marker SCD1. Scale bars, 50 μm. (**L**) FACS analysis of primary keratinocytes from A_K15CreER^{low}/R26RYFP mice comparing back skin 2 and 5 days following Cre activation. Table depicts fold changes of YFP+ cells coexpressing Itga6, CD34, Lrig1 or MTS24. (**M**) qRT–PCR of sorted cell populations comparing expression levels for non-bulge markers at 2 and 6 days following Tam pulse. (**N**) Model for SG regeneration by bulge-derived SCs. Individual YFP+ keratinocytes are located in the HF bulge and coexpress SC markers. After a chasing period of 3–5 days, bulge progeny are detected near the SG duct and SG and transit the MTS24/Plet1 compartment at the UI and the Lrig1 compartment of the JZ. Chasing SC progeny for additional 1 to 2 days results in YFP+ cells at the lower tip of the SG and further propagation of the cells. Traced bulge progeny coexpress Lrig1 at the inner periphery of the SG. Finally, the SG is renewed by bulge progeny and YFP+ keratinocytes coexpress the sebocyte marker SCD1.

Blimp1 as well as expression of Lrig1 and Lgr6 was increased in Plet1/MTS24 and YFP + keratinocytes at 6 days following Tam administration when compared with α6-integrin^{high}/CD34 + and YFP + HF bulge cells 2 days after Cre activation (Figure 4M). This demonstrates that YFP-labelled bulge progeny indeed transit through compartments characterised by Lgr6, Lrig1 and Blimp1 expression (Figure 4N).

Proliferation and migration of bulge SC

To directly track bulge SCs and study early steps of HF SC contribution for regeneration of the SG in more detail, a novel live cell imaging technique was developed. This involved isolation and *ex vivo* cultivation of epidermal whole mounts following Cre activation *in vivo* (Lu *et al*, 2007). As expected, the majority of labelled HF bulge cells analysed were quiescent. Intriguingly, time-lapse experiments of individual YFP + keratinocytes revealed that following SC division within the HF bulge one daughter cell moved directed towards the UI, whereas the second daughter cell remained within the bulge (Figure 5A and B). Cell division and dynamic movement towards the lower tip of the SG was also seen analysing YFP-labelled bulge progeny at the inner periphery of the SG (Supplementary Figure S5D). These data demonstrate that the process of SG renewal by HF bulge cells often involves cell division of SCs within the bulge followed by migration of one SC daughter out of the niche.

To analyse proliferation of bulge SCs in more detail, we have investigated EdU labelling of S-phase cells in telogen HFs. YFP + and EdU + two-cell clusters and, importantly, YFP/EdU double-positive cells could be localised to the bulge, the JZ and the SG (Figure 5C and G–I). Monitoring the process of SG renewal revealed that the inner periphery and the lower tip of the SG are repopulated before the entire SG is colonised by YFP + cells. Labelled cells within the SG were grouped according to their localisation at the lower tip (Ltip), on the top of the SG (top), the inner periphery (P) and central part (C) of the gland (Figure 5J and K). An increase in the number of positive cells (clone size) is detected within these different cell populations localised within the SG at later tracing time points. Interestingly, at the lower tip of the gland, clonal expansion is evident at day 8 following Cre activation and the size of clones are larger when compared with clones at the periphery, central part or top region of the SG. The results also suggest that the SG is repopulated by labelled HF bulge progeny at the inner periphery of the gland before cell clones expand at the lower tip of the gland (Figure 5K).

Development of ectopic SGs is coupled to de novo progenitor niche formation

To investigate the process of ectopic SG formation in more detail, expression of Plet1/MTS24 antigen and Lrig1 was analysed in whole mounts of K14ΔNLef1 mice. Lrig1 was strongly expressed in the JZ above the bulge of the HF and at the upper periphery of the SG. Additionally, Lrig1 was also localised below the bulge of the deformed HF at the periphery of newly formed SGs (Figure 6B) next to and overlapping with YFP + cells (Supplementary Figure S6A and B). The pattern of Plet1/MTS24 immunostaining was also altered. In addition to its expression at the UI and close to the periphery of the SG, Plet1/MTS24 was also defined to the periphery and ducts of branching *de novo* SGs (Figure 6C; Supplementary Figure S6C and D). Therefore, our data imply that induction of *de novo* SGs by over-expressing ΔNLef1 in mouse skin requires the establishment of SG progenitor niches (Figure 6D).

To further investigate the localisation of labelled bulge cells within K14ΔNLef1 mice, FACS experiments were performed. No significant change of the YFP + cell pool within the CD34 + bulge cells was seen when comparing samples from day 5 with day 2 after Cre activation (Supplementary Figure S6G and I). In contrast, an increase in labelled keratinocytes was detected within the cell compartment immunolabelled with MTS24 at 5 days of tracing (Supplementary Figure S6H and J). This result provides further proof for our observation that bulge progeny contribute to the formation of ectopic SG and the new progenitor compartments in K14ΔNLef1 mice. As expected, an overall increase within the number of YFP-labelled keratinocytes was monitored in K14ΔNLef1 mice (Supplementary Figure S6K).

In order to understand the molecular mechanism of ectopic SG formation in K14ΔNLef1 transgenic mice in more detail, qRT–PCRs on whole skin samples were conducted to compare an early (3 weeks; Supplementary Figure S6A and C) and late (3 months; Supplementary Figure S6B and D) time point of *de novo* SG development (Figure 6E and F). In a first set of experiments, expression levels of bulge markers were investigated. During early stages of ectopic SG formation, expression of some bulge markers including K15, NFATc1 and Sox9 was transiently increased when compared with wild-type skin samples. This could reflect the stage of activation and mobilisation of bulge SCs required for the formation of ectopic SGs. However, in older animals when ectopic glands are fully established, expression of bulge markers, for example K15, NFATc1, Sox9, LHX2, Tcf3, Tenascin C is significantly lower in transgenic mice compared with wild-type littermates (Figure 6E). Expression of K15 is reduced by $>60\%$ in K14ΔNLef1 mice and this observation was supported by immunofluorescence staining in which less K15 was detected when compared with controls (Figure 6A). Nevertheless, many YFP + cells were detected in the bulge region of deformed HFs in skin samples from transgenic mice, indicating remaining activity of the K15 promoter fragment driving Cre enzyme expression in a subpopulation of bulge cells. Interestingly, a transient increase in expression of marker molecules associated with SG lineage fate was seen at early stages of ectopic SG formation (Figure 6F). Blimp1 and K6a (Gu and Coulombe, 2008) are upregulated throughout the process of ectopic SG formation, whereas expression of the lipid modifying enzyme Elovl3 (Westerberg *et al*, 2004) is strongly elevated when the early steps of *de novo* SG formation are completed (Figure 6F). Previously, a recapitulation of the HF differentiation programme was seen in mouse models investigating the development of ectopic HFs (Lo Celso *et al*, 2004; Silva-Vargas *et al*, 2005). Therefore, our data suggest that the process of ectopic SG formation reapplies similar basic molecular signals that are essential for SG morphogenesis (Figure 6D).

Manipulating TCF/Lef1 signalling in the HF bulge results in abnormal SG formation

Our data clearly demonstrate that the HF bulge constitutes an important cellular reservoir for regeneration of SG tissue and formation of ectopic SGs. To investigate the function of HF

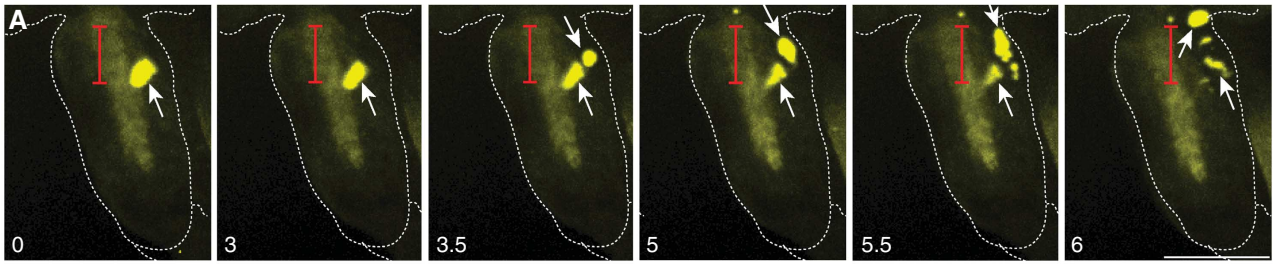

B

n=40 HF	Quiescent	Upward movement	Downward movement	Local movement
% of bulge cells	60	5	7.5	27.5

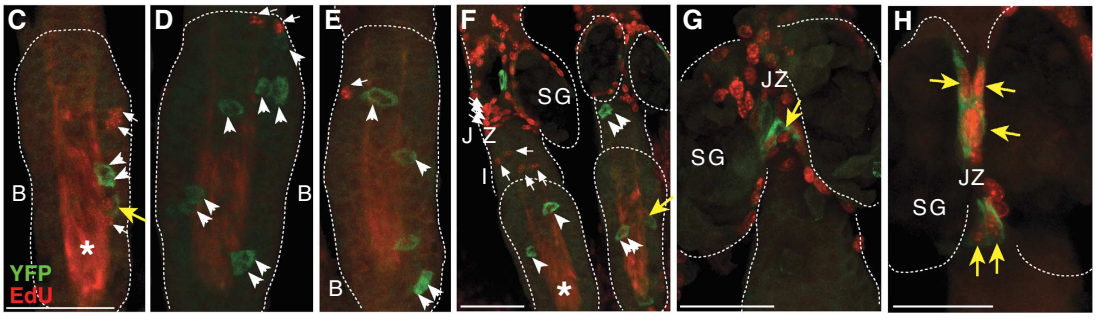

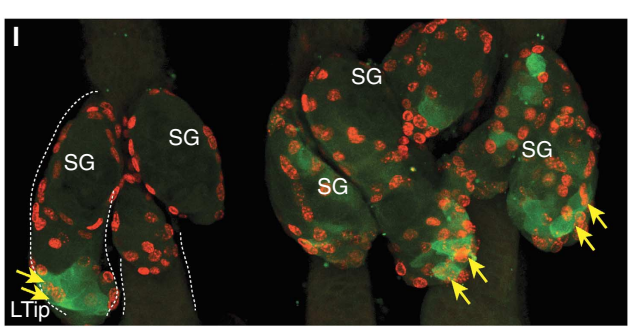

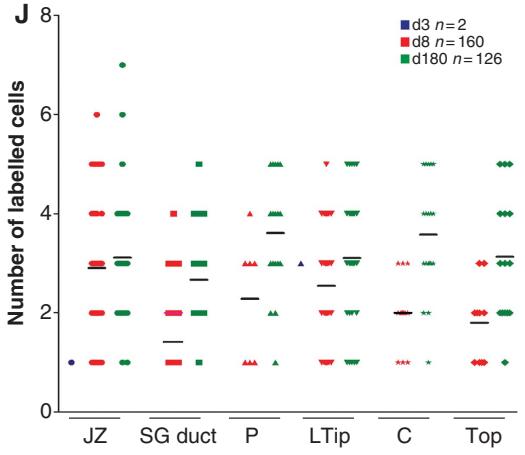

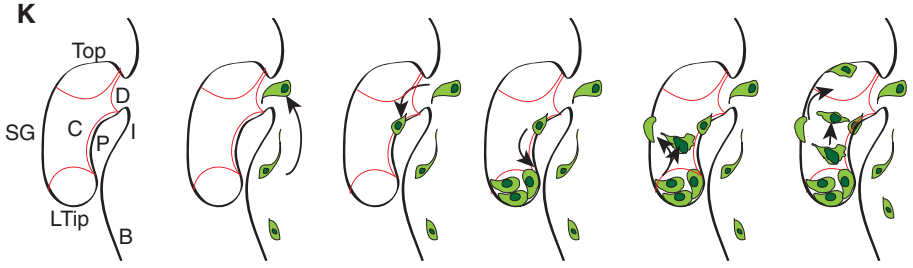

Figure 5 Characterisation and tracing of individual bulge SCs *ex vivo*. (**A**) Time-lapse studies on whole-mount explant cultures from A_K15CreER^{low}/Rosa26RYFP after Tam pulse *in vivo*. Monitoring of individual YFP + SCs for 6 h demonstrates cell division in the HF bulge and migration of one daughter cell towards the JZ and SG. Red bar marks distance covered by the cells. Scale bar, 70 μm. B, bulge; JZ, junctional zone; SG, sebaceous gland; UI, upper isthmus. (**B**) Summary of three independent experiments monitoring HF bulge cells applying live cell imaging on whole-mount explant cultures established from A_K15CreER^{low}/Rosa26RYFP mice following Tam administration. (**C**–**I**) Detection of EdU + S-phase cells (red, small arrows) and YFP + keratinocytes (arrow head) within the HF bulge (**C**–**E**), UI and JZ (**F**–**H**) as well as the SG (**I**) during telogen. Note EdU/YFP double-positive cells (yellow arrow). Asterisk marks unspecific staining of the hair channel caused by the dye. (**J**) Graph depicting size of labelled cell clones at the JZ and within different regions of the SG including SG duct, the periphery of the gland (P), lower tip of the SG (Ltip), centre region of the gland (**C**) and top of the SG (top, see also K for location) at 3, 8 and 180 days after Cre activation. (**K**) Scheme illustrating the process of SG renewal by bulge SC progeny.

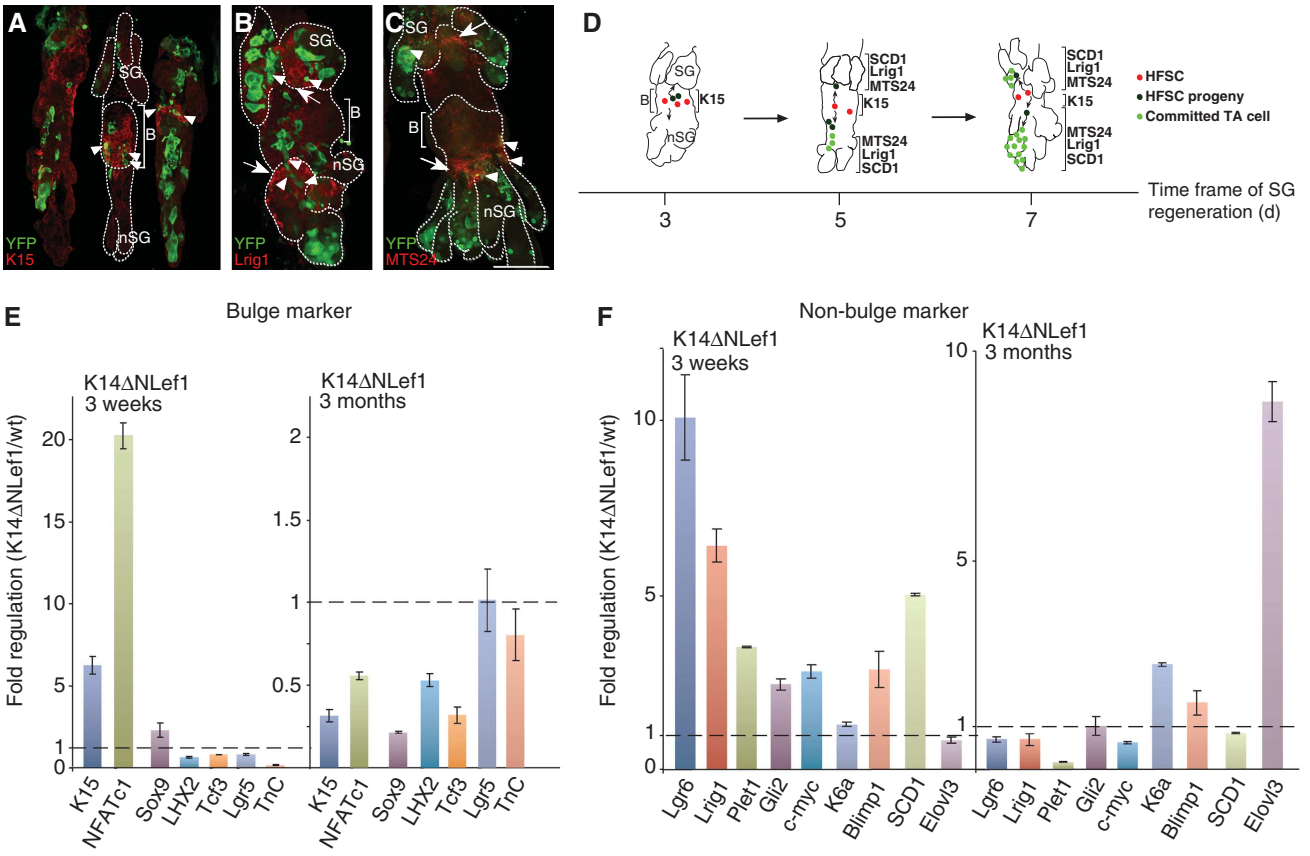

Figure 6 *De novo* SG formation by HF bulge cells is accompanied by establishment of new progenitor niches. (**A**–**C**) Detection of K15 (**A**, arrow heads), Lrig1 (**B**, arrows) and Plet1/MTS24 antigen (**C**, arrows) in K14ΔNLef1 mice. Establishment of new sebaceous progenitor niches at sites of *de novo* SG formation (**B**, **C** arrows). Individual YFP + cells transit the Lrig1 and MTS24 compartment (**B**, **C** arrow head). Scale bars, 50 μm. B, bulge; nSG, *de novo* sebaceous gland; SG, sebaceous gland. (**D**) Model for SG regeneration and *de novo* SG formation by HF-derived SCs. In K14ΔNLef1 transgenic mice bulge progeny contribute to SG regeneration and formation of *de novo* SGs along the deformed HF structures. These ectopic SGs are characterised by their own progenitor niches, which are positive for Plet1/MTS24 antigen and Lrig1. Bulge progeny transit through these distinct niches and finally differentiate into mature sebocytes. (**E**, **F**) Graph depicting gene expression levels of epidermal stem and progenitor markers (**E**) and marker molecules for SG commitment (**F**) analysed by qRT–PCR on the epidermis of 3-week-old and 3-month-old K14ΔNLef1 mice. Results are presented as fold regulation of mRNA from K14ΔNLef1 mouse epidermis compared with wild-type controls and are normalised to GapDH levels.

SCs during SG homoeostasis in more detail, the HF bulge compartment was specifically manipulated. Therefore, a transgenic mouse model over-expressing ΔNLef1 under control of the K15 promoter was generated. Three founder lines were established, which all exhibited low copy number of the transgene (1–8 copies). Mutant Lef1 protein was detected in individual cells within the HF bulge in K15ΔNLef1 mice but not in control littermates (Figure 7E). Whole mounts of adult transgenic mice exhibit a highly abnormal morphology of HFs and SGs. In particular, deformed HFs feature multiplication and enlargement of SGs (Figure 7B, D, E, G and H). Immunostaining for SCD1 further substantiated this observation of the dramatic increase in number of sebaceous lobules and sebocyte differentiation in K15ΔNLef1 mice (Figure 7A and B). Interestingly, Lrig1 was not only detected at the JZ and inner periphery of SGs as seen in control mice but also at the base of newly formed glands, resulting in an enlargement of the Lrig1 compartment (Figure 7C and D). The expression of marker molecules was analysed by qRT–PCR. These experiments demonstrate a general increase in sebaceous lineage marker molecules such as Lrig1, Lgr6, K6a and Gli2 in K15ΔNLef1 mouse epidermis. In contrast, expression of HF SC markers was not altered (Figure 7I). Surprisingly, bulge markers CD34 and K15 were not only detected within the HF bulge but also seen at SG ducts of duplicating SGs close to the JZ of the HF in transgenic mice, suggesting a more general function of mutant Lef1 for the regulation of HF morphology (Figure 7G and H). Thus, expression of ΔNLef1 within the HF SC compartment stimulated commitment of bulge progeny to sebocyte cell fate. These data further underline a crucial role of β-catenin/Lef1 signalling for directing lineage fate decisions within the mammalian epidermis.

Discussion

The mammalian epidermis is highly compartmentalised and recent data suggest that tissue homoeostasis is maintained by multiple classes of stem and progenitor cells (Yan and Owens, 2008). Among those, the HF bulge comprises the best-characterised SC compartment and previous studies provided compelling evidence that bulge SCs significantly contribute to HF regeneration and replenishment of the IFE after wounding in adult life (Ito *et al*, 2005, 2007; Cotsarelis, 2006). The genetic lineage tracing experiments presented

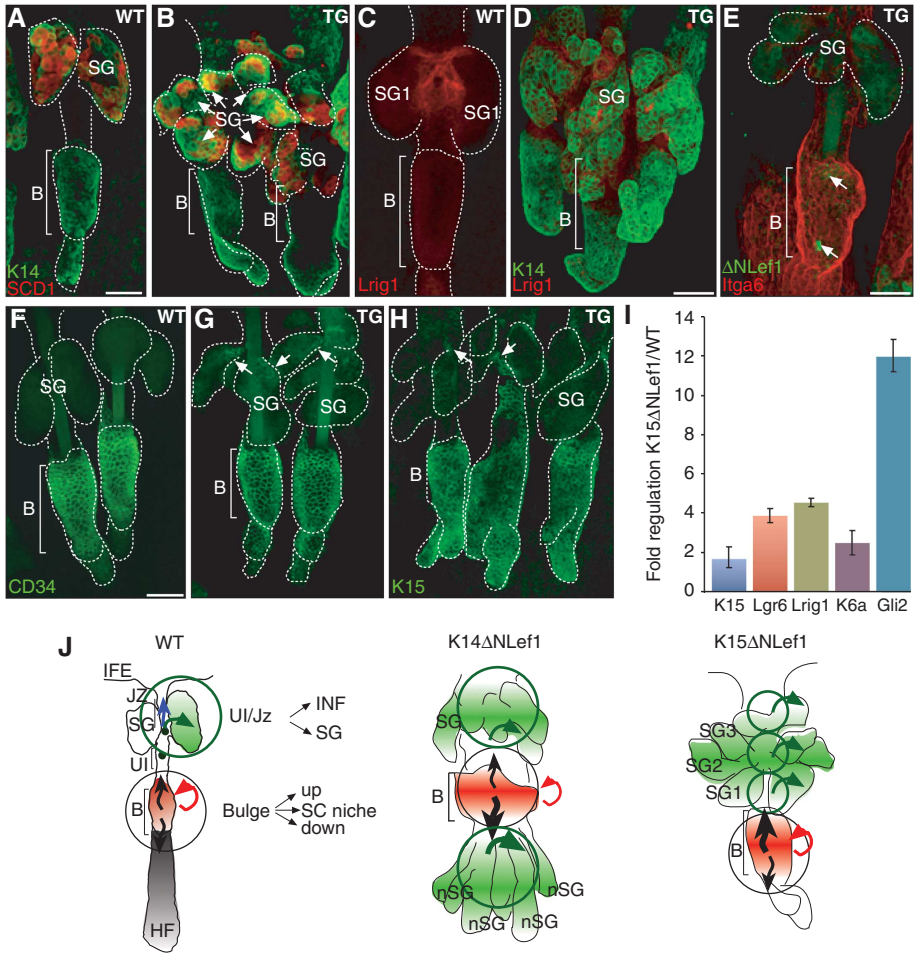

Figure 7 Manipulation of the HF bulge compartment results in expansion of the sebocyte lineage in K15ΔNLef1 mice. (**A**–**H**) Localisation of marker molecules SCD1 and K14 (**A**, **B**), Lrig1 (**C**, **D**), CD34 (**F**, **G**), K15 (**H**) and α6-integrin (Itga6) and transgene (**E**, arrows) in whole mounts of K15ΔNLef1 transgenic (**B**, **D**, **E**, **G**, **H**) and littermate controls (**A**, **C**, **F**). Note multiplication of SG structures in K15ΔNLef1 mice (arrows in **B**). Scale bars, 50 μm. (**I**) qRT–PCR results for lineage markers comparing keratinocytes of K15ΔNLef1 mice with littermate control cells shown as fold regulation after normalisation to GapDH levels. (**J**) Two cell fate determination centres are proposed. The HF bulge harbours SCs responding to at least three distinct signals to renew the HF, the SG or to replenish the HF SC compartment. At the JZ, progenitors are instructed to renew the SG or contribute to the cell pool of the infundibulum (INF). Additional determination centres (K14ΔNLef1) or expansion of the fate determination centre (K15ΔNLef1) is seen in transgenic mice upon interfering with Lef1 activity.

here demonstrate that progeny of adult HF SCs can give rise to different stem and progenitor populations of the pilosebaceous unit in mammalian skin. Thus, our data show that different stem and progenitor cell pools do not function autonomously in tissue renewal and homoeostasis but rather coexist in close interrelationship within a highly dynamic tissue.

In the process of SG renewal, SCs of the HF bulge generate progeny, which are competent to move upwards to replenish the SG and potentially the infundibulum of HFs. Our findings suggest the existence of two main cell fate determination centres within the pilosebaceous unit of mammalian skin (Figure 7J). The HF bulge constitutes one important region harbouring SCs competent to respond to at least three distinct signals to either renew the HF, the SG or to replenish the SC compartment. A second cell fate determination centre is localised at the JZ where SCs are instructed either to participate in SG renewal or to contribute to the cell pool of the infundibulum. Interference with functional TCF/Lef1 signalling results in additional fate determination centres (K14ΔNLef1 mice) or leads to expansion of existing sites for cell fate specification (K15ΔNLef1 mice) (Figure 7J). Importantly, our data do not rule out the possibility that non-bulge stem and progenitor cells might transit through other SC compartments, for example the HF bulge. Given the tremendous plasticity of basal keratinocytes in mammalian epidermis, this could be an underlying mechanism of tissue maintenance, especially following disturbances of epidermal homoeostasis.

The heterogeneity observed within the HF SC compartments highlights the importance of signals from the local environment for lineage commitment and differentiation within the tissue (Blanpain *et al*, 2004; Li and Clevers, 2010; Hsu *et al*, 2011). Our data reveal that one important prerequisite for establishing Lrig1 and Plet1/MTS24 positive cell populations is repression of β-catenin/Lef1 signalling activity. This is substantiated by our experiments analysing K14ΔNLef1 and K15ΔNLef1 transgenic mice. In these mouse models, expression of dominant negative Lef1 results in *de novo* formation of SGs and enlargement of existing glands.

Interestingly, the formation of ectopic SGs is accompanied by the development of MTS24/Plet1 and Lrig1 positive stem and progenitor cell niches (Figure 6D). This is in line with the findings made by other laboratories that Plet1 as well as Lrig1-expressing cells constitute crucial compartments enabling or even promoting sebocyte differentiation (Nijhof *et al*, 2006; Jensen *et al*, 2009).

Our results suggest that inhibition of TCF/Lef1 activity is also required to allow SG morphogenesis during early postnatal development of mouse epidermis. Presumably, β-catenin/TCF/Lef1 signalling is also blocked in the developing bulge area. Thus, the data point to a tight spatial and temporal control of TCF/Lef1 signalling activity within the pilosebaceous unit during morphogenesis. Our findings also disclose the importance of repression of TCF/Lef1 activity within the diverse stem and progenitor compartments located above the bulge to support SG lineage commitment.

Our lineage tracing experiments identified HF SCs as an important cellular source for ectopic SG formation and SG renewal during skin homoeostasis. However, bulge SCs are not the only source for SG renewal since other epidermal SCs, for example Lgr6+ isthmus cells have also been shown to repopulate the SGs (Snippert *et al*, 2010). Importantly, SG renewal by bulge SCs occurs during different phases of the hair cycle and is independent of HF regeneration. In contrast to the cyclic process of HF replacement, SG renewal occurs continuously. Therefore, distinct molecular mechanisms must exist to regulate activation of bulge SCs for cyclical HF regeneration and continuous SG renewal as well as replenishment of the SC pool as demonstrated in long-term studies. It is intriguing to speculate that different signals regulate SC mobilisation for either HF or SG/infundibulum renewal. In fact, the cellular mechanisms underlying HF and SG renewal are distinct. Subsequent to SC division within the HF bulge, SC progeny migrate towards the JZ and propagation of cells occurs mainly within the SG. In contrast, contiguous cell clones expanding from the HF bulge to the hair bulb are observed during anagen of hair regeneration (Zhang *et al*, 2010). While HF regeneration requires generation of large numbers of cells to establish a new hair, no expansion of the cell pool is required unless bulge progeny reach the area of the SG.

Our findings indicate that blocking TCF/Lef1 signalling activity promotes mobilisation of SCs for constant renewal of the SG and infundibulum of the HF. Previously, it has been suggested recently that intrinsic factors governing stemness might be different within the heterogeneous pool of bulge SCs (Hsu *et al*, 2011). This supports the idea that a subgroup of bulge SCs is preferentially targeted for mobilisation and SG renewal. An important future challenge for therapeutic purposes of tissue regeneration will be to identify the underlying signals and to unravel how SCs decipher and respond to these cues.

We provide novel insights into the cellular mechanism and temporal control of SG renewal during skin homoeostasis. In mouse tail skin, the SG is regenerated within 7 days by HF SCs during skin homoeostasis, indicating a high cellular turnover in the SG. From *in vivo* lineage tracing studies and live cell imaging of explant cultures of epidermal whole mounts we learned that the basal cell compartment located between the SG duct and lower tip of the SG is the first region populated by SC progeny (Figure 5K). This implies that keratinocytes at the lower tip of the SG are especially responsive to local signals promoting propagation and differentiation of basal cells. Alternatively, local signals at the lower tip of the gland might stimulate proliferation. Subsequently, residual undifferentiated basal keratinocytes and mature sebocytes are renewed by SC derivatives. Frequently, only one of the two SGs is regenerated after activation of individual HF SCs. This indicates that renewal of both SGs of tail skin requires activation of more than a single HF SC. Another possible explanation is that both SGs attached to one HF are not renewed simultaneously. This suggests that signals emanating from the JZ or the periphery of the SG instruct SC progeny to specifically renew one of the two glands.

To date, the cellular und molecular mechanisms of SG formation and regeneration are poorly understood. Previously, it has been shown that during morphogenesis of the pilosebaceous unit in embryonic mouse epidermis, HF SCs participate in the development of SGs. Genetic marking experiments using Sox9-Cre/R26R mice demonstrated active contribution of keratinocytes positive for the early HF SC marker Sox9 to the establishment of the SG lineage (Nowak *et al*, 2008). Interestingly, the molecular analysis of early stages of ectopic SG formation in K14ΔNLef1 mice revealed a transient increase in expression of bulge markers, including K15, NFATc1 and Sox9. These data imply that the formation of ectopic SGs requires activation and mobilisation of bulge SCs. It also suggests that the development of *de novo* SGs recapitulates stages of normal SG morphogenesis. Previously, it has been shown that for ectopic HF formation, similar molecular and cellular mechanisms are reapplied as seen during HF morphogenesis (Lo Celso *et al*, 2004; Silva-Vargas *et al*, 2005; Youssef *et al*, 2010).

The data presented here clearly demonstrate that HF SCs constitute an important source for *de novo* formation and continuous renewal of SGs in adult skin. Important questions for the future are the following: what are the molecular signals provided by the microenvironment regulating the diverse repertoire of SC responses and how are the different stem and progenitor cell compartments established and maintained within the tissue. Finally, it has been shown recently that bulge SCs are an important cellular source for skin cancer (Malanchi *et al*, 2008; Lapouge *et al*, 2011; Wang *et al*, 2011; White *et al*, 2011). Given the heterogeneity within the HF SC compartment, one of the key questions is if a subpopulation of the bulge is preferentially targeted for cancer initiation.

Materials and methods

Experimental mice

K15CreER(G)T2 was generated by inserting a 5-kb K15 promoter fragment (Liu *et al*, 2003) that was amplified and inserted using *SalI* restriction sites into the pK14CreER(G)T2 expression cassette after removal of the K14 regulatory sequence (Indra *et al*, 1999).

The K15ΔNLef1 DNA construct was assembled by removing the CreER(G)T2 sequence and inserting a myc-tagged ΔNLef1 DNA fragment (Niemann *et al*, 2002) into *EcoR1* sites of the K15CreER(G)T2 plasmid. Both constructs, K15CreER(G)T2 and K15ΔNLef1, were sequenced and *NotI* digestion was performed to linearise for microinjection. Injection resulted in the generation of eight transgenic K15CreER(G)T2 founder lines that were successfully identified applying convential PCR (K15for 5′-AGGTGTGC GGGCAGCTGTGTTTGT-3′; β-globrev 5′-GGACATCTTCCCATTCTAA

ACAACACCCTG-3′). Three low expressing K15ΔNLef1 founder lines were successfully established as detected by PCR (Lef1for 5′-TGTCC CTTGTATCACCATGGACC-3′ and Lef1rev 5′-CCAAAGATGACTTG ATGTCGGCT-3′ and K15for, β-globrev) and Southern blot.

K14ΔNLef1, R26RLacZ and R26RYFP Cre-reporter mice have been characterised previously (Soriano, 1999; Srinivas *et al*, 2001; Niemann *et al*, 2002). Cre recombinase was induced in K15CreER/R26RLacZ/YFP mice by injecting a single dose of 4 mg Tam (Sigma-Aldrich, Germany) intraperitoneally. In alternative experiments, 2.5 mg/day Tam was administered on 3 consecutive days. Specific LacZ/YFP and nuclear Cre staining pattern in the bulge region of the HF was detected in three founder lines of which two were used for all subsequent studies presented in this paper (A_K15CreER^{low} and C_K15CreER^{high}). Littermates of the same sex and genotype were used for administration of Tam or oil in control experiments.

To generate LRCs (Bickenbach *et al*, 1986; Bickenbach and Chism, 1998), mice (Pd10) were injected with 50 mg/kg bodyweight 5-bromo-2′-deoxyuridine (BrdU; Sigma-Aldrich) every 12 h for a total of four intraperitoneal injections as described previously (Braun *et al*, 2003). Mice were analysed for LRCs 6–8 weeks after injection. For analysis of cell proliferation, A_K15CreER^{low}/R26RYFP mice received up to eight doses EdU (0.3 mg/150 μl) following Tam treatment. EdU incorporation was assayed using EdU Click-it according to the manufacture's instructions (Invitrogen, Germany).

Experimental procedures were performed according to the institutional guidelines and animal licence given by the State Office North Rhine-Westphalia, Germany.

Antibodies

The following antibodies were used applying previously described protocols (Braun *et al*, 2003): K15 (Neomarkers LHK15 1:1000; Progen 1:1500), GFP (Abcam 1:2000; Molecular Probes 1:2500), K14 (Covance 1:6000); Cre (Covance 1:750), BrdU (OBT 1:500), CD34 (eBioscience clone RAM34 1:50), SCD1 (Santa Cruz S15 1:75), α6-integrin (BD Pharmingen CD49f 1:3000), Plet1/MTS24 (1:100, provided by R Boyd; Gill *et al*, 2002 and A Sonnenberg; Raymond *et al*, 2010), Lrig1 (R&D Systems 1:150), Lef1 (Cell Signaling 1:100), Tenascin C (1:1000 Chemicon). All secondary antibodies coupled to Alexa-488, Alexa-594, Cy5 or Cy3 were obtained from Molecular Probes.

Immunofluorescent analysis and β-galactosidase staining of epidermal whole mounts

Epidermal whole mounts of tail and back skin were isolated as described previously (Braun *et al*, 2003). Epidermal sheets isolated from both, tail and back skin, were fixed in 3.4% formaldehyde or 0.2% glutaraldehyde/2% formaldehyde for 2 h at RT. β-Galactosidase staining was conducted as described earlier (Liu *et al*, 2003). Samples were counterstained with haematoxylin and analysed by light microscopy (Leica DM 4000B). Immunofluorescent labelling of epidermal whole mounts was performed as described previously (Braun *et al*, 2003) and epidermal sheets were evaluated and visualised by confocal microscopy (Zeiss LSM711).

Ex vivo live cell imaging of epidermal whole mounts

Epidermal whole mounts were isolated from A_K15CreER^{low}/R26RYFP following a single injection of Tam (5 mg/0.2 ml sunflower oil) and preparation was done as previously described (Braun *et al*, 2003). For live cell imaging of YFP-labelled vital bulge cells ($n=40$), tissue samples were cultivated at 32°C and 5% CO_2 and the Perkin-Elmer Ultra view vox confocal imaging system in conjunction with a Nikon Eclipse Ti microscope and a Nikon Plan Fluor ×20/0.75 objective was used. Scans are presented as *z*-projections. Pictures were taken every 30 min over the course of up to 22 h with a Hamatsu C9100-50 camera (1000 × 1000 pixel) at a binning of 2. Image analysis was performed with the Volocity 5.3.2. Build 0 imaging software (Perkin-Elmer, UK).

Statistical analysis and three-dimensional reconstructions

Epidermal whole mounts of Tam-treated A_K15CreER^{low}/R26RLacZ mice and littermate controls were analysed for LacZ-positive cells at 3 and 8 days following Cre activation ($n=3$ per tracing time point). LacZ+ cells were counted and classified according to localisation of labelled cells within the pilosebaceous unit, namely bulge only (B); bulge, SG duct and SG; and SG and SG duct. In all experiments, labelling efficiency was >50%. s.d. was calculated and *P*-value for labelled HF bulge cells per pilosebaceous unit between 3 days and 6 months of tracing ($n=3$ mice/time point) was determined by Student's *t*-test. Classification of hair cycle stages was performed according to the morphological criteria as described by Muller-Rover *et al* (2001). Confocal *z*-stack projections were rendered using Volocity software.

qRT–PCR analysis

Total RNA from freshly isolated and sorted primary keratinocytes was purified using Trizol (Invitrogen, Germany). The QuantiTect Reverse Transcriptase Kit (Qiagen, Germany) was employed for cDNA synthesis according to the manufacturer's instructions. Quantitative real-time PCR analyses were conducted using RT^2 RT SYBR Green qPCR Master Mix (SuperArray Bioscience Cooperation, USA) and a StepOnePlus real-time PCR system (Applied Biosystems). The following PCR conditions were applied: 10 min 95°C initial denaturation, cyclic denaturation at 95°C for 15 s followed by an annealing step at 60°C for 1 min. Primer pairs were designed as shown in Supplementary Table 1 and also see Jaks *et al* (2008). Fold differences between primary keratinocytes derived from K14ΔNLef1 or K15ΔNLef1 mice as well as age and sex-matched wild-type control animals were calculated based on the $\Delta\Delta C_t$ method, adjusted to GapDH expression and are depicted as fold change normalised to wt expression. For FACS-sorted cells, the ΔC_t method was applied and changes were adapted to 18S RNA expression and normalised to α6-integrin (Itga6) positive keratinocytes.

Supplementary data

Supplementary data are available at *The EMBO Journal* Online (http://www.embojournal.org).

Acknowledgements

We thank D Fehrenschild, S Moll, H Nöbel, G Peinkofer (Center for Molecular Medicine Cologne), A Schauss (CECAD imaging facility, Cologne), M Höhne (Department of Internal Medicine IV, University of Cologne) for excellent technical support and C Niessen and T Krieg (Department of Dermatology, University of Cologne) for critical reading of the manuscript and helpful discussions. We are grateful to G Cotsarelis (University of Pennsylvania), P Chambon (IGBMC Strasbourg) and R Boyd (Monash University) for reagents and K Braun (Centre for Cutaneous Research London), S Tiede (Department of Dermatology, University of Lübeck) and D Owens (Colombia University, NY) for experimental advise. We acknowledge funding by the German Cancer Aid and German Research Foundation (SFB 572 and SFB 829).

Author contributions: CN designed the project and wrote the paper. CN and MP designed the experiments. MP performed most of the experiments and the data analysis. HB, AK, SJ, GR and PS performed a significant amount of the experimental work.

Conflict of interest

The authors declare that they have no conflict of interest.

References

Alonso L, Fuchs E (2006) The hair cycle. *J Cell Sci* **119:** 391–393

Bickenbach JR, Chism E (1998) Selection and extended growth of murine epidermal stem cells in culture. *Exp Cell Res* **244:** 184–195

Bickenbach JR, McCutecheon J, Mackenzie IC (1986) Rate of loss of tritiated thymidine label in basal cells in mouse epithelial tissues. *Cell Tissue Kinet* **19:** 325–333

Blanpain C, Fuchs E (2006) Epidermal stem cells of the skin. *Annu Rev Cell Dev Biol* **22:** 339–373

Blanpain C, Fuchs E (2009) Epidermal homeostasis: a balancing act of stem cells in the skin. *Nat Rev Mol Cell Biol* **10:** 207–217

Blanpain C, Lowry WE, Geoghegan A, Polak L, Fuchs E (2004) Self-renewal, multipotency, and the existence of two

cell populations within an epithelial stem cell niche. *Cell* **118:** 635–648

Braun KM, Niemann C, Jensen UB, Sundberg JP, Silva-Vargas V, Watt FM (2003) Manipulation of stem cell proliferation and lineage commitment: visualisation of label-retaining cells in wholemounts of mouse epidermis. *Development* **130:** 5241–5255

Clayton E, Doupé DP, Klein AM, Wintin DJ, Simons BD, Jones PH (2007) A single type of progenitor cell maintains normal epidermis. *Nature* **446:** 185–189

Clevers H (2006) Wnt/beta-catenin signaling in development and disease. *Cell* **127:** 469–480

Cotsarelis G (2006) Epithelial stem cells: a folliculocentric view. *J Invest Dermatol* **126:** 1459–1468

Cotsarelis G, Sun TT, Lavker RM (1990) Label-retaining cells reside in the bulge area of pilosebaceous unit: implications for follicular stem cells, hair cycle, and skin carcinogenesis. *Cell* **61:** 1329–1337

Depreter MG, Blair NF, Gaskell TL, Nowell CS, Davern K, Pagliocca A, Stenhouse FH, Farley AM, Fraser A, Vrana J, Robertson K, Morahan G, Tomlinson SR, Blackburn CC (2008) Identification of Plet-1 as a specific marker of early thymic epithelial progenitor cells. *Proc Natl Acad Sci USA* **105:** 961–966

Doupé DP, Klein AM, Simons BD, Jones PH (2010) The ordered architecture of murine ear epidermis is maintained by progenitor cells with random fate. *Dev Cell* **18:** 317–323

Fuchs E, Horsley V (2008) More than one way to skin. *Genes Dev* **22:** 976–985

Ghazizadeh S, Taichman LB (2001) Multiple classes of stem cells in cutaneous epithelium: a lineage analysis of adult mouse skin. *EMBO J* **20:** 1215–1222

Gill J, Malin M, Hollander GA, Boyd R (2002) Generation of a complete thymic microenvironment by MTS24(+) thymic epithelial cells. *Nat Immunol* **3:** 635–642

Greco V, Chen T, Rendl M, Schober M, Pasolli HA, Stokes N, Dela Cruz-Racelis J, Fuchs E (2009) A two-step mechanism for stem cell activation during hair regeneration. *Cell Stem Cell* **4:** 155–169

Gu LH, Coulombe PA (2008) Hedgehog signaling, keratin 6 induction, and sebaceous gland morphogenesis: implications for pachyonychia congenita and related conditions. *Am J Pathol* **173:** 752–761

Haegebarth A, Clevers H (2009) Wnt signaling, Lgr5, and stem cells in the intestine and skin. *Am J Path* **174:** 715–721

Han G, Li AG, Liang YY, Owens P, He W, Lu S, Yoshimatsu Y, Wang D, Ten Dijke P, Lin X, Wang XJ (2006) Smad7-induced beta-catenin degradation alters epidermal appendage development. *Dev Cell* **11:** 301–312

Horsley V, Aliprantis AO, Polak L, Glimcher LH, Fuchs E (2008) NFATc1 balances quiescence and proliferation of skin stem cells. *Cell* **132:** 299–310

Horsley V, O'Carroll D, Tooze R, Ohinata Y, Saitou M, Obukhanych T, Nussenzweig M, Tarakhovsky A, Fuchs E (2006) Blimp1 defines a progenitor population that governs cellular input to the sebaceous gland. *Cell* **126:** 597–609

Hsu Y, Pasolli HA, Fuchs E (2011) Dynamics between stem cells, niche, and progeny in the hair follicle. *Cell* **144:** 92–105

Indra AK, Warot X, Brocard J, Bornert JM, Xiao JH, Chambon P, Metzger D (1999) Temporally-controlled site-specific mutagenesis in the basal layer of the epidermis: comparison of the recombinase activity of the tamoxifen-inducible Cre-ER(T) and Cre-ER(T2) recombinases. *Nucleic Acids Res* **27:** 4324–4327

Ito M, Liu Y, Yang Z, Nguyen J, Liang F, Morris RJ, Cotsarelis G (2005) Stem cells in the hair follicle bulge contribute to wound repair but not to homeostasis of the epidermis. *Nat Med* **11:** 1351–1354

Ito M, Yang Z, Andl T, Cui C, Kim N, Millar SE, Cotsarelis G (2007) Wnt-dependent *de novo* hair follicle regeneration in adult mouse skin after wounding. *Nature* **447:** 316–320

Jaks V, Barker N, Kasper M, van Es JH, Snippert HJ, Clevers H, Toftgard R (2008) Lgr5 marks cycling, yet long-lived, hair follicle stem cells. *Nat Genet* **40:** 1291–1299

Jensen KB, Collins CA, Nascimento E, Tan DW, Frye M, Itami S, Watt FM (2009) Lrig1 expression defines a distinct multipotent stem cell population in mammalian epidermis. *Cell Stem Cell* **4:** 427–439

Jensen UB, Yan X, Triel C, Woo SH, Christensen R, Owens DM (2008) A distinct population of clonogenic and multipotent murine follicular keratinocytes residing in the upper isthmus. *J Cell Sci* **121:** 609–617

Lapouge G, Youssef KK, Vokaer B, Achouri Y, Michaux C, Sotiropoulou PA, Blanpain C (2011) Identifying the cellular origin of squamous skin tumours. *Proc Natl Acad Sci USA* **108:** 7431–7546

Li L, Clevers H (2010) Coexistence of quiescent and active adult stem cells in mammals. *Science* **327:** 542–545

Liu Y, Lyle S, Yang Z, Cotsarelis G (2003) Keratin 15 promoter targets putative epithelial stem cells in the hair follicle bulge. *J Invest Dermatol* **121:** 963–968

Lo Celso C, Prowse DM, Watt FM (2004) Transient activation of beta-catenin signalling in adult mouse epidermis is sufficient to induce hair follicles but continuous activation is required to maintain hair follicle tumours. *Development* **131:** 1787–1799

Lu Z, Hasse B, Bodo E, Rose C, Funk W, Paus R (2007) Towards the development of a simplified long-term organ culture method for human scalp skin and its appendages under serum-free conditions. *Exp Dermatol* **16:** 37–44

Lyle S, Christofidou-Solomidou M, Liu Y, Elder DE, Albelda S, Cotsarelis G (1999) Human hair follicle bulge cells are biochemically distinct and possess an epithelial stem cell phenotype. *J Investig Dermatol Symp Proc* **4:** 296–301

Malanchi I, Peinado H, Kassen D, Hussenet T, Metzger D, Chambon P, Huber M, Hohl D, Cano A, Birchmeier W, Huelsken J (2008) Cutaneous cancer stem cell maintenance is dependent on beta-catenin signalling. *Nature* **452:** 650–653

Merrill BJ, Gat U, DasGupta R, Fuchs E (2001) Tcf3 and Lef1 regulate lineage differentiation of multipotent stem cells in skin. *Genes Dev* **15:** 1688–1705

Morris RJ, Liu Y, Marles L, Yang Z, Trempus C, Li S, Lin JS, Sawicki JA, Cotsarelis G (2004) Capturing and profiling adult hair follicle stem cells. *Nat Biotechnol* **22:** 411–417

Muller-Rover S, Handjiski B, van der Veen C, Eichmuller S, Foitzik K, McKay IA, Stenn KS, Paus R (2001) A comprehensive guide for the accurate classification of murine hair follicles in distinct hair cycle stages. *J Invest Dermatol* **117:** 3–15

Niemann C (2006) Controlling the stem cell niche: right time, right place, right strength. *Bioessays* **28:** 1–5

Niemann C, Owens DM, Hulsken J, Birchmeier W, Watt FM (2002) Expression of DeltaNLef1 in mouse epidermis results in differentiation of hair follicles into squamous epidermal cysts and formation of skin tumours. *Development* **129:** 95–109

Niemann C, Owens DM, Schettina P, Watt FM (2007) Dual role of inactivating Lef1 mutations in epidermis: tumor promotion and specification of tumor type. *Cancer Res* **67:** 2916–2921

Niemann C, Watt FM (2002) Designer skin: lineage commitment in postnatal epidermis. *Trends Cell Biol* **12:** 185–192

Nijhof G, Braun KM, Giangreco A, van Pelt C, Kawamoto H, Boyd RL, Willemze R, Mullenders LH, Watt FM, de Gruijl FR, van Ewijk W (2006) The cell-surface marker MTS24 identifies a novel population of follicular keratinocytes with characteristics of progenitor cells. *Development* **133:** 3027–3037

Nowak JA, Polak L, Pasolli HA, Fuchs E (2008) Hair follicle stem cells are specified and function in early skin morphogenesis. *Cell Stem Cell* **3:** 33–43

Panteleyev AA, Rosenbach T, Paus R, Christiano AM (2000) The bulge is the source of cellular renewal in the sebaceous gland of mouse skin. *Arch Dermatol Res* **292:** 573–576

Raymond K, Richter A, Kreft M, Frijns E, Janssen H, Slijper M, Praetzel-Wunder S, Langbein L, Sonnenberg A (2010) Expression of the orphan protein Plet-1 during trichilemmal differentiation of anagen hair follicles. *J Invest Dermatol* **130:** 1500–1513

Rhee H, Polak L, Fuchs E (2006) Lhx2 maintains stem cell character in hair follicles. *Science* **312:** 1946–1949

Schneider MR, Paus R (2009) Sebocytes, multifaceted epithelial cells: lipid production and holocrine secretion. *Int J Biochem Cell Biol* **42:** 181–185

Silva-Vargas V, Lo Celso C, Giangreco A, Ofstad T, Prowse DM, Braun KM, Watt FM (2005) Beta-catenin and Hedgehog signal strength can specify number and location of hair follicles in adult epidermis without recruitment of bulge stem cells. *Dev Cell* **9:** 121–131

Snippert HJ, Haegebarth A, Kasper M, Jaks V, van Es JH, Barker N, van de Wetering M, van den Born M, Begthel H, Vries RG, Stange DE, Toftgard R, Clevers H (2010) Lgr6 marks stem cells in the hair follicle that generate all cell lineages of the skin. *Science* **327:** 1385–1389

Soriano P (1999) Generalized lacZ expression with the ROSA26 Cre reporter strain. *Nat Genet* **21:** 70–71

Srinivas S, Watanabe T, Lin CS, William CM, Tanabe Y, Jessell TM, Costantini F (2001) Cre reporter strains produced by targeted insertion of EYFP and ECFP into the ROSA26 locus. *BMC Dev Biol* **1:** 4

Taylor G, Lehrer MS, Jensen PJ, Sun TT, Lavker RM (2000) Involvement of follicular stem cells in forming not only the follicle but also the epidermis. *Cell* **102:** 451–461

Trempus CS, Morris RJ, Bortner CD, Cotsarelis G, Faircloth RS, Reece JM, Tennant RW (2003) Enrichment for living murine keratinocytes from the hair follicle bulge with the cell surface marker CD34. *J Invest Dermatol* **120:** 501–511

Tumbar T, Guasch G, Greco V, Blanpain C, Lowry WE, Rendl M, Fuchs E (2004) Defining the epithelial stem cell niche in skin. *Science* **303:** 359–363

Vidal VP, Chaboissier MC, Lutzkendorf S, Cotsarelis G, Mill P, Hui CC, Ortonne N, Ortonne JP, Schedl A (2005) Sox9 is essential for outer root sheath differentiation and the formation of the hair stem cell compartment. *Curr Biol* **15:** 1340–1351

Wang GY, Wang J, Mancianti M, Epstain Jr EH (2011) Basal cell carcinomas arise from hair follicle stem cells in ptch$^{+/-}$ mice. *Cancer Cell* **19:** 1–11

Watt FM, Lo Celso C, Silva-Vargas V (2006) Epidermal stem cells: an update. *Curr Opin Genet Dev* **16:** 518–524

Wend P, Holland JD, Ziebold U, Birchmeier W (2010) Wnt signaling in stem and cancer stem cells. *Semin Cell Dev Biol* **21:** 855–863

Westerberg R, Tvrdik P, Undén AB, Månsson JE, Norlén L, Jakobsson A, Holleran WH, Elias PM, Asadi A, Flodby P, Toftgard R, Capecchi MR, Jacobsson A (2004) Role for ELOVL3 and fatty acid chain length in development of hair and skin function. *J Biol Chem* **279:** 5621–5629

White AC, Tran K, Khuu J, Dang C, Cui Y, Binder SW, Lowry WE (2011) Defining the origins of Ras/p53-mediated squamous cell carcinoma. *Proc Natl Acad Sci USA* **108:** 7425–7430

Yan X, Owens DM (2008) The skin: a home to multiple classes of epithelial progenitor cells. *Stem Cell Rev* **4:** 113–118

Youssef KK, Van Keymeulen A, Lapouge G, Beck B, Michaux C, Achouri Y, Sotiropoulou PA, Blanpain C (2010) Identification of the cell lineage at the origin of basal cell carcinoma. *Nat Cell Biol* **12:** 299–305

Zhang YV, Cheong J, Ciapurin N, McDermitt DJ, Tumbar T (2009) Distinct self-renewal and differentiation phases in the niche of infrequently dividing hair follicle stem cells. *Cell Stem Cell* **5:** 267–278

Zhang YV, White BS, Shalloway DI, Tumbar T (2010) Stem cell dynamics in mouse hair follicles. *Cell Cycle* **9:** 1504–1510

Zouboulis CC, Baron JM, Bohm M, Kippenberger S, Kurzen H, Reichrath J, Thielitz A (2008) Frontiers in sebaceous gland biology and pathology. *Exp Dermatol* **17:** 542–551

